Research Paper

Ultrasonic P- and S-Wave Reflection and CPT Soundings for Measuring Shear Strength in Soil Stabilized by Deep Lime/Cement Columns in Stockholm Norvik Port

Per LINDH[(1),(2)], Polina LEMENKOVA[(3)]

[(1)] *Department of Investments, Technology and Environment, Swedish Transport Administration*
Malmö, Sweden, e-mail: per.lindh@trafikverket.se

[(2)] *Faculty of Engineering, Department of Building and Environmental Technology*
Division of Building Materials, Lund University
Lund, Sweden, e-mail: per.lindh@byggtek.lth.se

[(3)] *École Polytechnique de Bruxelles, Laboratory of Image Synthesis and Analysis (LISA)*
Université Libre de Bruxelles (ULB)
Brussels, Belgium

[*]Corresponding Author e-mail: polina.lemenkova@ulb.be

In this research project, the measurements of the ultrasonic P- and S-waves and seismic cone penetration testing (CPT) were applied to identify subsurface conditions and properties of clayey soil stabilized with lime/cement columns in the Stockholm Norvik Port, Sweden. Applied geophysical methods enabled to identify a connection between the resistance of soil and strength in the stabilized columns. The records of the seismic tests were obtained in the laboratory of Swedish Geotechnical Institute (SGI) through estimated P- and S-wave velocities using techniques of resonance frequency measurement of the stabilized specimens. The CPT profiles were used to evaluate the quality of the lime/cement columns of the reinforced soil by the interpretation of signals. The relationship between the P- and S-waves demonstrated a gain in strength during soil hardening. The quality of soil was evaluated by seismic measurements with aim to achieve sufficient strength of foundations prior to the construction of the infrastructure objects and industrial works. Seismic CPT is an effective method essential to evaluate the correct placement of the CPT inside the column. This work demonstrated the alternative seismic methods supporting the up-hole technology of drilling techniques for practical purpose in civil engineering and geotechnical works.

Keywords: civil engineering; soil stabilization; compressive strength; cement; lime; seismic waves.
PACS: 81.40.Cd; 81.40.Ef; 62.20.Qp; 83.50.Xa; 45.70.Mg; 92.40.Lg; 81.40.Lm; 62.20.M-.
2000 MSC: 76Axx; 74Exx; 74Fxx.

Acronyms

ASCII – American Standard Code for Information Interchange,
CPT – cone penetration testing,
DSM – deep soil mixing,
FEM – finite element method,
LKD – lime kiln dust,
OPC – ordinary Portland cement,
OCR – overconsolidation ratio,
QL – quick lime,
SPT – standard penetration test,
SGI – Swedish Geotechnical Institute,
UCS – uniaxial compressive strength.

1. Introduction

1.1. Background

Stabilization of soil is a fundamental issue in civil engineering. Prior to engineering and construction works, weak soils should be stabilized using binders

such as cement (Bache *et al.*, 2022; Chen *et al.*, 2021; Lindh, Lemenkova, 2022f), lime (Kichou *et al.*, 2022; Chand, Subbarao, 2007), slag (Lindh, Lemenkova, 2021a) or others (Mirzababaei *et al.*, 2018). Compared to native soil, stabilized mixture exhibits the improved properties such as increased strength, enhanced elastic modulus and stiffness (Madhyannapu *et al.*, 2010; Sundary *et al.*, 2022), improved liquefaction resistance (Ito *et al.*, 1994). Other advantages include the reduced porosity, permeability and shrinkage (Tonini de Araújo *et al.*, 2023; El-Rawi, Awad, 1981; Åhnberg, 2003), decreased swell potential in soils prone to freeze-thaw cycles (Shihata, Baghdadi, 2001; Bin-Shafique *et al.*, 2011; Orakoglu *et al.*, 2017), increased resistance against the impacts from moisture and temperature (Zhang *et al.*, 2020; Kim *et al.*, 2012). Such improved properties make soil suitable to earthworks and ensure the safety of constructions and civil infrastructure systems (roads, communications, tunnels, highways). This especially concerns the high plasticity expansive clay soils of Sweden.

Existing methods of soil stabilization can be divided into two broad categories: traditional methods of soil stabilization and evaluation of strength (Trhlíková *et al.*, 2012; Lindh, Lemenkova, 2022b; Heidarizadeh *et al.*, 2021) and advanced seismic methods using non-destructive techniques of acoustical soundings (Varma *et al.*, 2022; Foti *et al.*, 2002; Lindh, Lemenkova, 2021b; Garcia-Suarez *et al.*, 2021). The traditional methods of evaluation of the improvements in the stabilized soil include the uniaxial tests (Avci, Mollamahmutoğlu, 2016; Lapointe *et al.*, 2012; Xu, Yi, 2021) or triaxial (Alvarado, Coop, 2012) using laboratory equipment which are robust and widely applied approaches. However, they have certain limitations and disadvantages. Firstly, these methods are destructive, i.e., tested specimens are crashed after the experiments. Secondly, these tests are not applicable to be carried out on the fissured clay. Moreover, the uniaxial compressive strength (UCS) may be not precise for soils with the angle of shearing resistance not equal to zero where the shear strength is not equal to half the compressive strength. On that basis, the use of the applied methods of data analysis based on mathematical modelling (Jefferies, 2022) is better applicable for evaluation of soil characteristics.

The applied geophysical methods have been widely used in the context of seismic and acoustical tests. These are based on the evaluation of the velocities of P- and S-waves penetrating the soil (Safaee *et al.*, 2022; Lindh, Lemenkova, 2022d, Foti, Lancellotta, 2004). Other examples include the Rayleigh–Ritz method which evaluates the free vibration characteristics in the ground (Sonkar, Mittal, 2022; Jones, 1958) or attenuation of waves through the

evaluation of vibration over time (Colombero *et al.*, 2015). Several experimental papers have been published on the application of wave velocity to evaluate soil parameters. Among these, Santamarina and Cascante (1998) report on the existing relationship between the wave propagation and the inherent properties of the materials, such as fabric, mineralogical structure, surface roughness, size of particles and angularity, which control soil strength and stiffness.

Ultrasonic and bender element tests used to measure the elastic modulus and evaluate the rigidity of soil as the shear modulus from compression waves are reported in (Amaral *et al.*, 2011) with a case of sand samples stabilized by cement. The use of the free-free resonant column tests in combination with the UCS tests has also proved to be applicable to the sand-cement mixtures for measurement of the electrical resistivity and mechanical properties of the stabilized soil (Rusati *et al.*, 2020). Other examples in this category include measuring the shear wave velocity during the penetration testing (Hepton, 1989), and determining the dynamic shear modulus of the ground, independent of Poisson's ratio (Abbiss, 1981).

The cone penetration testing (CPT) is an effective method of soil investigation and identification of the subsurface conditions. Originally developed in the Netherlands in the 1930s and initially named as the Dutch cone test (Brouwer, 2007; McCallum, 2014), it has nowadays numerous applications in geotechnical engineering, such as prediction of liquefaction resistance (Olsen, 2018; Fitzgerald, Elsworth, 2012; Saye *et al.*, 2021), evaluation of strength (Price *et al.*, 2016; Jamiolkowski *et al.*, 2003), and measuring excess pore pressure (Sully, Campanella, 1991; Elsworth *et al.*, 2006). Nowadays, CPT is one of the most used methods for measurements of the geotechnical properties of soil. For instance, the applications of CPT for estimation of deformation modulus of soil (Shahien, Farouk, 2013; Benz Navarrete *et al.*, 2022) and characterising soil liquefaction potential by Guan *et al.* (2022) are worth mentioning. The related methods include, for instance, estimating the cone penetration resistance for analysis of the soil compressibility (Bisht *et al.*, 2021).

The deep soil mixing (DSM) method is an in situ stabilization of soil in which soil is mixed with binders, typically cementitious materials, lime, slag or similar stabilizing agents. Over the last decades, there has been a rise in research into the DSM methods, as a response to the appearance of novel construction practices and equipment in addition to the existing general techniques of drilling in cored boreholes (Hepton, 2015). These are the techniques of stabilizing the unsaturated expansive subsoils at the moderate active depths (Madhyannapu, Puppala, 2014; Madhyannapu *et al.*, 2009), or settlement control in the highway embankment (Archeewa *et al.*, 2011).

The cases of the reinforced embankments supported by the DSM cement columns are presented by LAMBRECHTS et al. (2012) for stability and the settlement control, BERGADO et al. (2008) with computed permeability and the compressibility ratio and the consolidation of the columns and clay, and YAPAGE et al. (2014) with evaluated settlements, excess pore-water pressures and lateral deformations in a strain-softening behavior of the deep cement columns.

Cohesive soil with high moisture content and fine-grained structure, such as clays, silts or loams, are best stabilized by lime and cementitious binders. As a result, soil has enhanced parameters which result in the increased strength, reduced permeability and compressibility. However, the engineering properties of soil stabilized by the DSM method depend on various factors including the following ones: the original characteristics of the native soil, the types and the amount of binders, technical and operational parameters defined by the construction types, curing time, depth, external parameters such as temperature and moisture, and loading conditions.

In this paper, we propose a framework of novel applications of the DSM and seismic methods to address the problem of the evaluation of strength of the expansive clay stabilized with lime/cement columns. The methodology includes the in-situ fieldwork and laboratory based measurements and modelling. The CPT soundings were performed in the area of the Stockholm Norvik Port. The resistance and strength of soil in the stabilized columns was evaluated by seismic tests. A method of resonant frequency measurements of the compressional wave velocities was embedded into these tests. We applied the alternative seismic methods supporting the up-hole technology of the drilling techniques. This enabled to evaluate the pressure by the S- and P-waves for lime/cement columns. We report the results of seven columns with performed CPT probing (ACS155, ACW151, ADA147, ADC148, AEG35, AEE356, and AEA358). We evaluated the relationship between the P- and S-waves which showed the gain in strength.

1.2. Objectives and goals

The background to the project is the need to correctly evaluate the quality of the lime/cement columns in terms of strength and homogeneity in the region of the Stockholm Norvik Port – a new deep sea port of Sweden in the Baltic Sea. Norvik consisted of a bay until the beginning of the 1980s, surrounded by a hilly strip of land and a mountainous island. Nowadays, this area is largely reconstructed for the container terminal of the Stockholm Norvik Port. The Stockholm Norvik Port is an important port transporting cargo in the capital with a direct connection to other regions of Sweden in the Baltic Sea and northern Europe. The

sustainable and efficient operation of the infrastructure in the port modalities requires safe constructions on the stabilized ground. Therefore, the objectives of this work are to determine the strength properties of soil stabilized by lime/cement columns using the CPT. The CPT was evaluated as a test method for the stabilization of soil prior to construction works. The practical goal of this work is to connect the laboratory tests and field measurements to obtain a better and safer optimization of the binders in terms of types and proportions for soil stabilization. In the response to these needs, the aim is to evaluate seismic methods for evaluating the strength of the soil, stabilized by various binders.

2. Methods

2.1. Fieldwork

In this project, the field investigations were carried out during the period of 7–10 November 2016 in Norvik. The technical equipment included the multipurpose drilling rig GEORIG – Model 607 used for soundings. The GEORIG – 607, developed by Geotech AG, was selected as a proper instrument for drilling, since it is equipped with all the necessary devices for soil rock drilling, Swedish weight sounding, dynamic sounding, standard penetration test (SPT) and CPT. The GEORIG 607 was anchored with a screw to achieve the sufficient holding force, Fig. 1.

Fig. 1. Process of CPT sounding in Norvik area.
Photo source: Per Lindh.

During the construction of a gas storage facility in Nynäshamn, the bay was filled with the explosives from the construction. The filling was carried out by the tipping masses from several fronts, which meant that the large volumes of clay were enclosed in the blast-stone filling. The two large areas, northern and southern ones, were identified and used as study areas, filled with clay up to 30 m. Previously, several geotech-

nical field investigations in this area were carried out in 1982, 2008, 2010, and 2011 with technical details reported clay properties and stabilization (ERIKSSON, 2015). The requirements for the lime/cement columns in this project were set on the achieving of a minimum in situ shear strength of 150 kPa after 28 days of curing period. To ensure this, the requirement for the laboratory packed samples is set to at least 200 kPa. Several mixtures of the stabilized soil that contained cement, quicklime and the lime kiln dust (LKD) met the requirements of at least 200 kPa after 28 days of storage. Since the in situ temperature in the columns is partly dependent on the type and the amount of binder, the laboratory tests differed from the fieldwork results, especially when the laboratory cured samples were stored at 7°C in a climate room where the cooling is significantly greater than in in-situ conditions.

2.2. Laboratory tests

2.2.1. Test chamber

Prior to the laboratory tests, the test chamber was well examined and documented in terms of technical conditions for natural soil collected in the Stockholm Norvik port. The laboratory measurements on the stabilized soil were carried out using seismic tests of P-wave and flexwave (shear wave) velocities that evaluated the strength of the stabilized samples. Seismic tests were carried out as a reference to the measurements in the field.

2.2.2. Determination of the material parameters

The soil stabilized in this project included natural clay with parameters reported in Figs. 2 and 3. The overall density values vary in the range of 1.40 to 2.00 t/m³ in the depth up to 25 m (Fig. 2, right). The values of both the natural water ratio (W_N) of soil and the yield strength (W_L) vary from 40 to 100% (Fig. 2). The density mostly varies between 1.5 to 1.7 tons per m³. The corrected shear strength, c_u-korr, is mainly between 5 and 15 kPa and the clay is low to medium, in terms of sensitivity.

2.2.3. Binders

Three different binders were used in this study: 1) ordinary Portland cement (OPC) of type CEM II/A; 2) burnt lime, or quick lime (QL); 3) LKD. These binders were selected due to their effectiveness and applicability, as tested in previous studies (LINDH, LEMENKOVA, 2022c). Using these three general types of binders, nine combinations of the blended mixes were fabricated and tested. The mixing quantities corresponded to 80, 100, and 120 kg of binder per m³ of clay. To evaluate binder combinations for stabilization using the deep mixing method, the experimental setup using the simplex centroid design was used following the existing methodology (LINDH, LEMENKOVA, 2022e). Hence, various percentage of the three binders was tested in an experiment which consists of a triangle with pure binders in the corners and a mixture of two binders along the triangle's stripes.
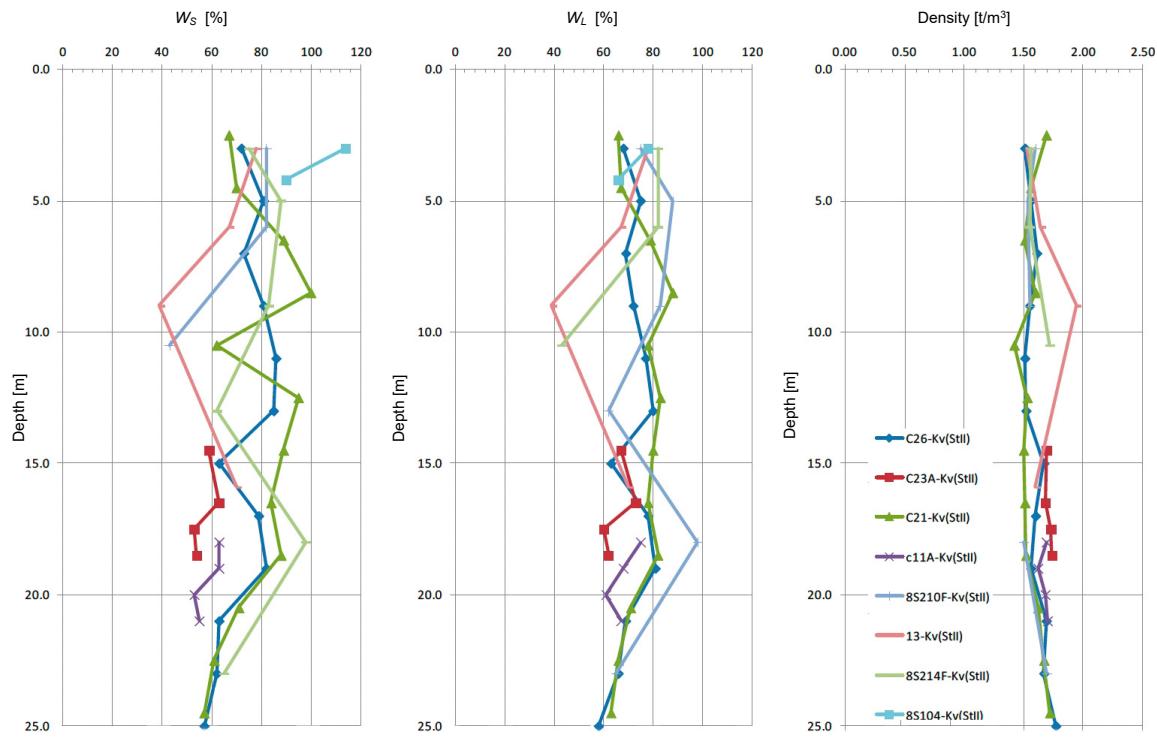

Fig. 2. Variations in water ratio, yield strength and density in natural clay over depth.
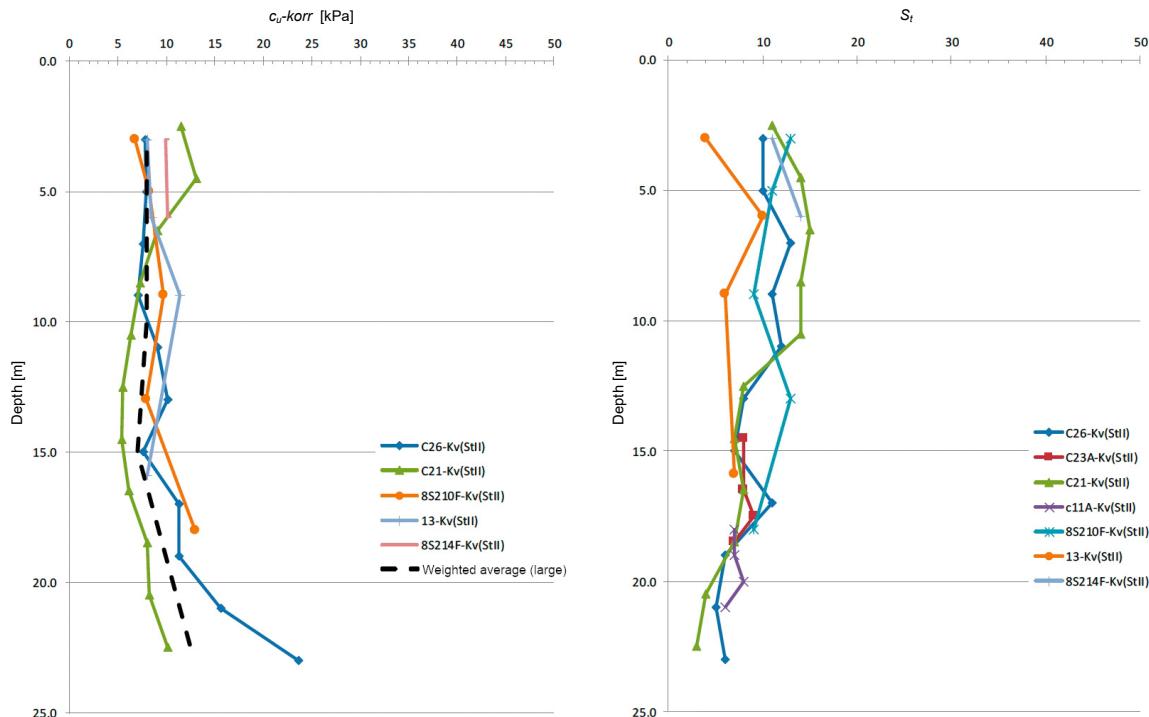
Fig. 3. Shear strength and sensitivity changed over depth for the large clay area.

A combination of all the three binders was tested experimentally inside the triangle with a total binder content as a constant. The trial surface in a three-factor simplex centroid is structured as a triangle with the corners of the triangle representing 100% of one binder and the centre of the triangle corresponds to 33% of the three different binders. The mutual ratio between the binders varies depending on where in the triangle the test point is located. These tests were carried out according to the laboratory quality handbook of the Swedish Geotechnical Institute (SGI) (document 29a, rev c). Each trial point was performed as a double trial. The points on the lower edge of the triangle correspond to either a pure binder (cf., CEM II/A or QL), or, alternatively, as a mixture of 50% CEM II/A and 50% QL. Testing the proportions and the amount of binders was carried out on clay collected from the test excavation sites carried out at Norvik.

The curing times for the samples was determined as 7, 14, 21, and 28 days with measurements of strength performed on the reference days. Some extra specimens were evaluated on the 80th day of curing. In addition, extra reference tests were carried out for calibration of seismic measurements in relation to the compressive strength at 7 and 14 days. The experimental setup was performed as a three factor simplex centroid with a restriction limitation of the LKD content which was increased up to 50%. The purpose of the statistical trial planning is to minimise the number of trials in view of the large amount of materials that should be tested in real conditions (dozens tons of soil) and to statistically optimise the binder blends. At the same time, the experimental planning maintains the statistical significance and ensures that both positive and negative interactions between the binder components are detected.

2.3. Seismic tests

The natural resonance frequency (f_n) is the number of oscillations per second (Hz) in a test body that is allowed to oscillate and swing freely without damping. The lowest resonant frequency is called the fundamental mode. All natural resonance frequencies can be physically related to the elastic constants, E-modulus (E) and transverse contraction number or seismic velocities such as primary wave (P-wave) and secondary wave (S-wave or shear wave). For specimens with a length twice the diameter $(L/D \geq 2)$, the one-dimensional (1D) wave propagation velocity was calculated using Eq. (1):

$$V_{P1D} = 2Lf_d, \qquad (1)$$

where f_d is a damped resonance frequency.

Seismic measurements were performed as a resonance frequency measurement of the P-wave and S-wave, Fig. 4. The advantage of the P-wave measurements is that these can be carried out on the specimens while they harden in the sleeve so that the sleeve does not significantly affect the measurements. The disadvantage of measuring the P-wave is that it is strongly affected when soil becomes saturated with water, when

Sr goes towards one. When soil is saturated with water, the measurement of P-wave velocity of soil sample is affected by the included water for which the P-wave velocity is about 1500 m/s. Necessarily, this may lead to the incorrect and biased results. However, this bias is not significant in the laboratory-made specimens, because these cannot be saturated with water without a very high pressure.

Measuring the shear wave instead enables to solve this problem in cases when it is not affected by high water saturation levels. However, the measurement of the true shear wave is more difficult with a free-free resonant column setup. A common way to evaluate a shear wave, although not entirely accurate, is to measure the bending mode, i.e., flex mode or transverse mode (VERÁSTEGUI-FLORES *et al.*, 2015). According to this approach, the shear wave velocity is underestimated by approximately 5% for a specimen with a slenderness factor of 2 (where slenderness is a ratio of length/diameter) and a = 0.2. The setup for measuring the flex mode is shown in Fig. 4.
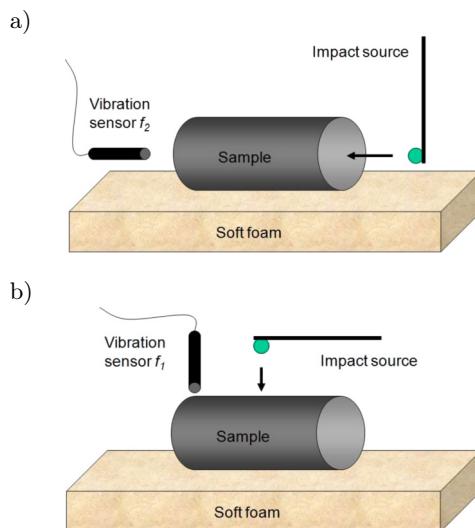
Fig. 4. Setup of test measurements: a) P-wave frequency of a sample body by a free-resonance column approach; b) flex wave frequency (f_f) of a sample body using a free resonance frequency of column.

The evaluation of the shear wave velocity is calculated according to Eq. (2):

$$V_s = 2Lf_f. \tag{2}$$

To measure true shear waves in a laboratory, it is necessary to use bending elements. However, this methodology is cumbersome and requires a long time. To solve this problem, a new methodology has been tried at the SGI to evaluate the torsional mode aimed at a better calculation of the shear wave, Fig. 5. However, this approach is not yet sufficiently tested and should be verified with more measurements and analysis using the finite element method (FEM) to check that the correct mode is evaluated.
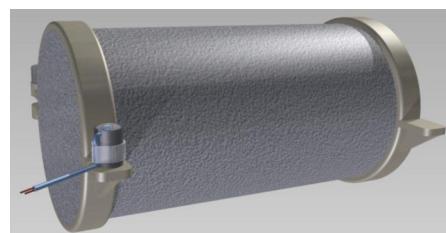

Fig. 5. Sketch of the experimental setup for measuring torsion mode according to the free-free resonance column principle.

To evaluate how both the P-wave velocity and shear strength develop with time, reference soil samples were fabricated. The reference samples consisted of a standard recipe consisting of 50% OPC and 50% QL. The advantage of the use of P-wave velocity in the laboratory tests is that it can also be measured on soil specimens stored in sleeves. However, in such case, the length of the sleeves must be equal to the length of the sample. Otherwise, the resonance frequency of the sleeve is measured additionally, which biases the results. The binder quantities were chosen corresponding to 80, 100, and 120 kg/m³. After 7 days of curing, the P-wave velocity and shear strength were evaluated on the two samples with each binder quantity. This was repeated on days 14, 21, 28, and 80, respectively. This type of correlation has previously been used for the surface-stabilized specimens and indicated robust results (LINDH, LEMENKOVA, 2022a). The choice of 80 days was based on the degree days to compare with the 28 day strength of samples stored at 20°C. A better procedure would have been to use maturity numbers (M_T) instead of the degree days.

2.4. Seismic CPT

The CPT probe is performed according to the standard SS-EN ISO 22476-1:2012 for subsurface exploration. The reason for using seismic CPT is that in this method, a peak pressure and both seismic values obtained from the P-wave (compression wave) and S-wave (shear wave) are evaluated. During the CPT probing, a cylindrical probe with a cross-sectional area of 1000 mm² is driven, where the probe has a tip angle of 60°. The pushing of the instrumented cone into the ground was performed at a continuous rate of 2.0 cm/s. During the CPT, the force required to drive the probe down was measured by the mechanical measurements to evaluate the penetration resistance of soil when pushing a cone with a conical tip into the soil. The casing friction was measured through a backlash coupling, to distinguish it from the tip pressure. The pore pressure generated during the pushing was measured using a filter system located behind the probe tip, and the friction force gauge was used to measure the friction ratio between the sleeve friction and the

tip resistance, which was measured as a percentage, see the scheme in Fig. 6.
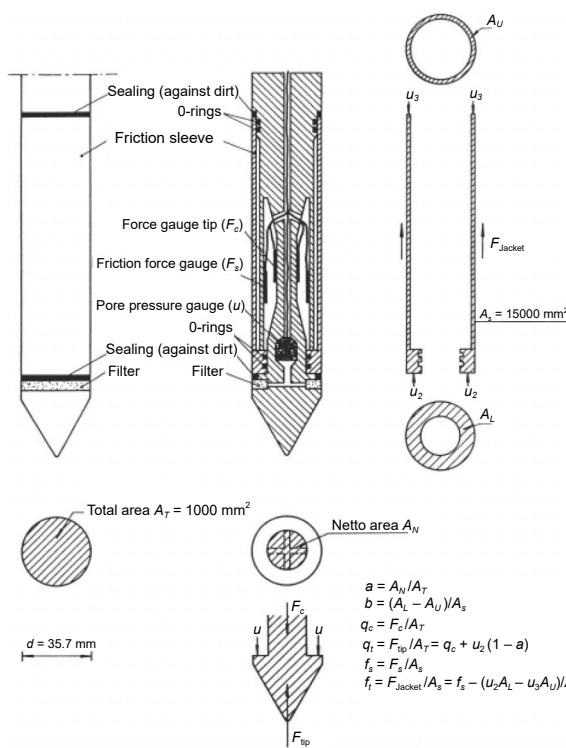
Fig. 6. Schematic diagram of the composition of a CPT probe. Modified after: SGI Information 15.

During the tests, the tip resistance (MPa) is recorded as a force required to push the tip of the cone through soil. It is determined as the force per unit area obtained by dividing the measured force by the cross-sectional area of the tip. This peak pressure is denoted as q_c if the pore pressure is not taken into account and q_t if the value is corrected taking into account error sources from the effects of the soil pores. In a special case, when $u \approx 0$ or is negligible, q_c becomes q_t. The CPT probe is reported and registered in standard protocols using Conrad software, as shown in Fig. 16. The sounding was carried out following the traditional methods of the CPT sounding. The specifics of the fieldwork is that at the depth where seismic measurements were carried out, the CPT sounding was paused, while the P- and S-wave measurements started.

The measurements used a sledgehammer which was connected with an earth cable to the measuring equipment to generate shear and compression waves. At the start of seismic measurements, the problems arose with the signal, which could be traced to motor vibrations and transmission between the drill chuck and drill steel. This was resolved by releasing the drill chuck and shutting down the motor of the drill track carriage. The CPT soundings were not performed at the centre of the columns, to avoid the disturbances at the centre arising from the column installation itself.

The Seismic CPT included the measurements of shear and compression waves, in addition to the regular CPT soundings. The measurements were performed using a series-connected device that was placed between the CPT probe and the probing rods. The measurements were performed by stopping the CPT probe at the required level of 25 m. Alternatively, the systems with continuous measurements can also be used. In such cases, measurements should be stopped after splicing the bars.

There are two different principles of seismic measurements.

The first principle is based on the two rounds of accelerometers (A1 and A2) with a fixed distance between them, Fig. 7a. The accelerometers measure the x-, y-, and z-directions, where y-direction identifies the pitch. This principle calculates the penetration speed based on the time measurement between the first
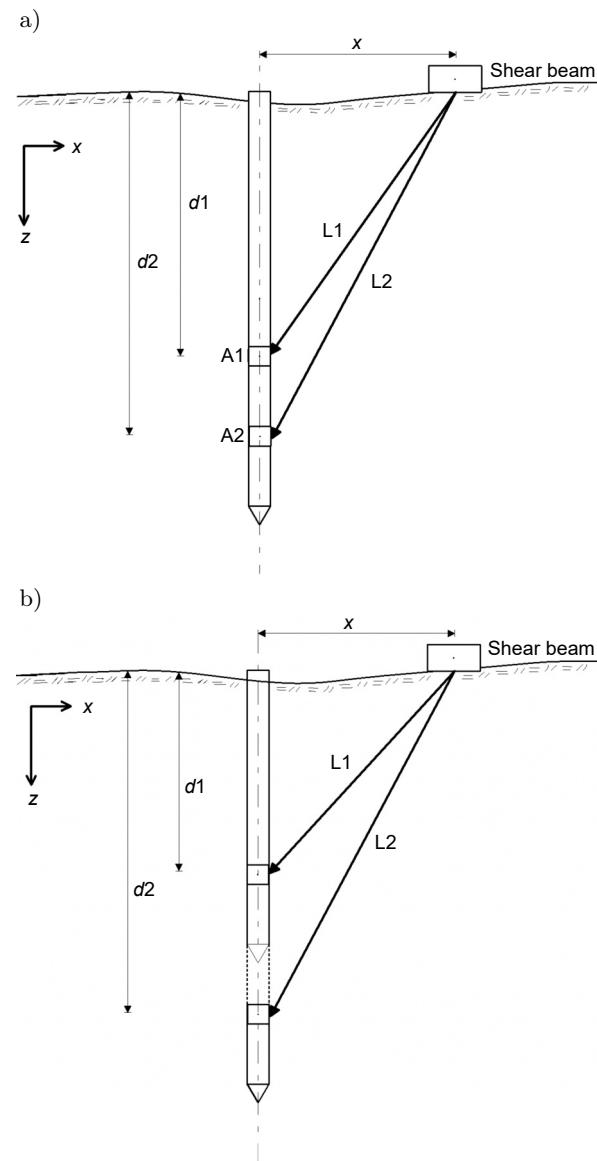

Fig. 7. Schematic diagram of a seismic CPT probe with: a) dual accelerometers; b) one accelerometer.

wave propagation to accelerometers 1 and 2. Therefore, this method is sometimes referred to as "true-time", since the fixed distance between the accelerometers provides a safer determination of the time difference and thus a precise determination of the ground running speed, Fig. 7a. As the distance between the accelerometers is constant, the speed can be calculated directly.

The second principle is based on carrying out the measurements with only one set of the accelerometers with registration in three directions (x, y, and z). The measurement is first performed at one level, after which the CPT probing continues and a new measurement is performed at the next level, Fig. 7b. In this case, the accelerometer measures signals in the x-, y-, and z-directions, where y-direction identifies the pitch. This method is often called "pseudo-time", as the distance is based on the two different measurements where the difference in depth is taken from the CPT logging. First, a depth measurement $d1$ is performed, after which the probe is pressed down to the depth $d2$ to continue with the next measurement, Fig. 7b.

An alternative to the above is to combine the limestone probe with the seismic CPT approach. In cases where a more reliable determination of the soil properties is needed, we recommend the application of these alternatives. An alternative to using the seismic CPT is the up hole technique for quality control of the lime/cement columns. This methodology involves the installation of the pipe in or near the centre of the column which means that the pipe is installed using lime/cement column machine. Such technology was developed for installation of the measuring pipes and reported in previous investigations of the SGI in SD Technical Report 35. This can be a good solution to quick and easy installation of the pipes for drilling.

After the initial hardening of soil specimens, the measurements of soil strength were performed using the following techniques. On the top of the lime/cement column, four accelerometers were installed, positioned with a 90° angle between the accelerometers. The test included the evaluation of the P- and S-wave sources which were lowered into the pipe to the target depth, after which the probe was clamped as a "packer", the waves were excited and their velocity was measured, Fig. 8. The experiment was repeated in the directions where the accelerometers are placed. After the measurements are finished on one level, the probe is moved up to the next level, where the measurements continued in an iterative manner.

The advantage of this method is that it ensures a good contact between the columns and the accelerometers. Besides, the excitation wave and the location of the seismic source are very well defined. Moreover, an additional advantage is that the measurements can be carried out by one person without costs for drilling rigs, which significantly decreases the financial
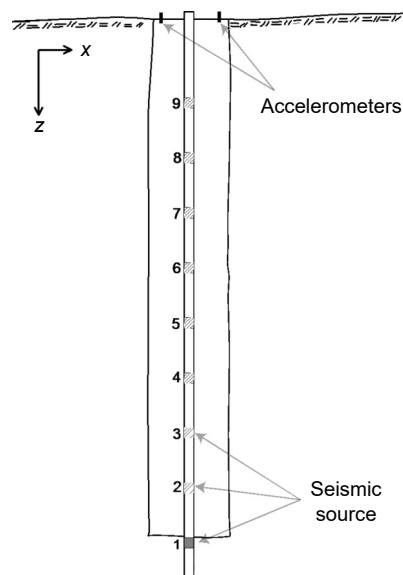

Fig. 8. Schematic sketch of the "up hole" measurements of the lime/cement column.

costs in the project. However, there are also some disadvantages of this method which should be mentioned. The quality of the columns is usually the worst at the top. This can be solved either by excavating the top or by attaching the accelerometers at a deeper level. Another disadvantage compared to the seismic CPT is that it is necessary to decide in advance which columns are to be measured. Therefore, in order to obtain a direct comparison with the limestone probe, a slotted pipe can be used for the up hole measurements, after which a normal test with the limestone probe is carried out.

2.5. Shear strength evaluation from CPT

The evaluation of the CPT probe has been performed using Conrad software, version 3.1. In a fine-grained soil, shear strength is primarily evaluated as the net peak pressure. An alternative method for clays is to use the generated pore overpressure. The empirical relationships developed for the conditions of Swedish soil are based on the evaluated dataset containing field measurements and laboratory data from a variety of soil types collected in Sweden. For natural clay soil, the relationship between the net peak pressure and shear strength is sensitive to the yield strength of soil (W_L) and to some extent also to the degree of the overconsolidation ratio (OCR), which is described according to Eq. (3):

$$c_u = \frac{q_t - \sigma_{\nu 0}}{13.4 + 6.65 W_L} \left(\frac{\text{OCR}}{1.3} \right)^{-0.2}. \qquad (3)$$

In cases where values of the yield strength of clay are missing, Eq. (4) is used instead:

$$c_u \approx \frac{q_t - \sigma_{\nu 0}}{N_{kt}}, \qquad (4)$$

where N_{kt} (empirical confactor) is set to 16.3 for clay. In the Conrad evaluation software, N_{kt} is denoted by N_{11}. For a binder-stabilized soil, there is not the same amount of the empirical evidence and therefore, not much literature about which value of N_{kt} should be used. There are recommendations that N_{kt} values should be set between 17–20 for a stabilized soil (LARSSON, 2017; MAKUSA *et al.*, 2014). Furthermore, there are limitations in evaluation of the firmness in different layers of highly layered soil, because the tip pressure is affected from the above as the underlying layer at a distance of 5 to 20 times tip diameters. To evaluate a firmer layer in a loose soil using this method, the thickness of the layer should be between 4.4–4.7 m. In the opposite case, with a looser layer in a firmer soil, the thickness of soil layer should be between 0.2 to 0.4 m. This means that the diapason of weakness in a lime/cement column can easily be missed in the CPT evaluation. This becomes the most important issue for the evaluation of a lime/cement column reinforcement in the shear zone.

In a binder-stabilized soil, the pozzolanic reactions take place and continue for many months, therefore the properties of the stabilized soil (texture, structure, strength, etc.) partly change over time. For instance, change in the texture of clay is based on the exchange of ions in the clay and change in the water ratio. The ion exchange is described by the lyotropic series:

$$\text{Li}^+ < \text{Na}^+ < \text{H}^+ < \text{K}^+ < \text{NH}_4^+ \ll \text{Mg}^{++} < \text{Ca}^{++} \ll \text{Al}^{+++}.$$
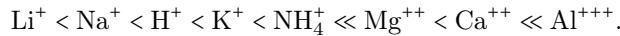
The change in the structure of the clay mineral is shown in Fig. 9.
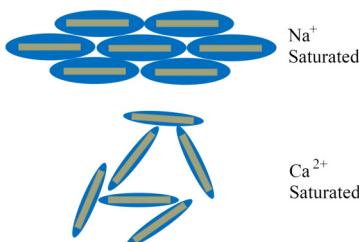
Fig. 9. Change in texture and water-holding of clay as it moves from a sodium saturated system to a calcium-saturated system.

Thus, the stabilized clay has a change in plasticity, yield strength, and other parameters. The degree of change depends both on the type of clay mineral and on the type of binder. The changes in the structure of the stabilized clay mean that the empirical relationships that exist between the tip pressure and shear strength of the original non-stabilised clay differ for a stabilized clay. To evaluate samples cured at different temperatures, soil specimens can be compared between laboratory-processed samples cured in climate rooms at 7°C and those fabricated in situ under the differ-

ent temperature conditions. In this case, the maturity number M_T is defined according to Eq. (5):

$$M_T = [20 + (T - 20) \times K]^2 \times \sqrt{t}, \qquad (5)$$

where T – temperature (°C), t – time (days), K – material-dependent empirical constant. The material-dependent empirical constant K is calculated by curing samples at different temperatures, e.g., 7°C and 20°C. The samples were then measured with the resonance frequency measurement at different time intervals. The results from the seismic measurements were used to fit the curves so that they coincide, i.e., different values of K are used, after which the curves are compared. A common value of K accepted in this study is 0.5, although literature has also shown $K \approx 1$ (ÅHNBERG, HOLM, 1987).

3. Results and discussion

3.1. Results of the lime/cement column recipes

3.1.1. Strength determination

In the testing of binder combinations, a reference recipe of the OPC CEM II/A and QL were used in a mutual ratio of 50/50%. The evaluated shear strength for reference samples at different curing times is reported in Fig. 10. Here the quantities of binders represented 80, 100, and 120 kg of binders per m³ of clay. The samples were stored in a climate room with a temperature of 7°C. The results show the higher strength in the samples stabilized with 120 kg of binders per m³ of clay, while the lowest values for the 80 kg of binder. Thus, on the 80th day of stabilization, the highest values of shear strength reached 430, 445, and 465 kPa for soil mixtures stabilized with 80, 100, and 120 kg of binders, respectively. This indicates that the amount of binders directly affects the strength of soil in the final output.
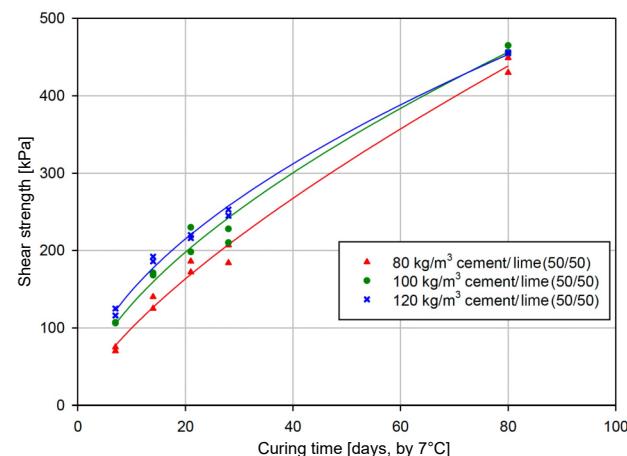

Fig. 10. Shear strength as a function of curing time for test specimens stabilized by a combination of CEM II/A and burned lime (50/50).

In order to evaluate the effects of different combinations of binders on shear strength of the stabilized soil material, a test setup was used supported by Pareto diagrams, Fig. 11. The Pareto chart shows the effect of the different components of binders on the stabilization results with the achieved significance value $p = 0.05$. For a binder amount at $80 \, \text{kg/m}^3$, the results show a clear positive interaction between various components (OPC, QL, and LKD) in a binder combination, Fig. 11. The direct and positive interaction means that binder components generate a higher strength than can be expected from a linear regression between the effects of the individual binders. The model has an explanation rate of 95%, i.e., it explains 95% of the variations in shear strength. The setup of test for binder amount of $100 \, \text{kg/m}^3$ clay contains an extended number of tests. For comparison with other amounts of binders, the analysis was performed with the same number of trial points as for 80 and 120 kg of binders, respectively. The results of this analysis show a lower positive interaction between the binders. However, this should be compared with the result from the analysis of the extended trials. In a trial setup with more internal trial points, the resolution increases, and the degree of the explanation rate of the model increases as well, from 95% to 97.5%. The extended model shows a greater interaction between various binder components for a mix amount corresponding to 120 kg of binder per m^3 of clay. At this mix amount, the positive interaction of the binder components was insignificant. The degree of explanation of the response surface, according to the Response Surface Methodology (RSM) (MYERS, MONTGOMERY, 1995; MONTGOMERY, 1996) was 98%.
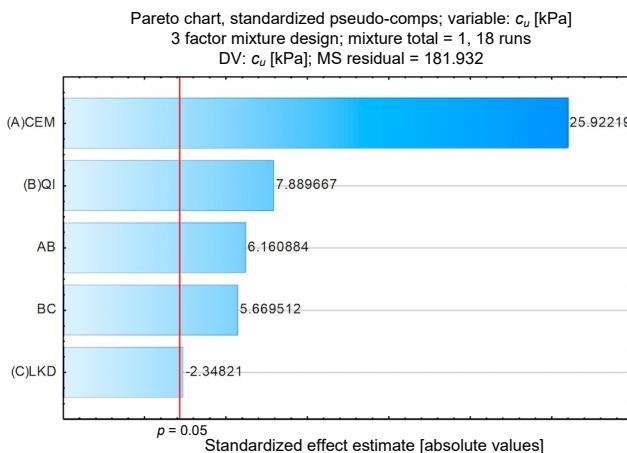
Fig. 11. Pareto chart showing the effects of binders on soil stabilization with the significance level 0.05 for a mixture of 80 kg of binders per m^3 of soil.

3.1.2. Seismic measurements

Seismic measurements included the evaluation of the velocity of P-waves, according to the resonance frequency method. The P-wave is an axial wave passing through the cylindrical specimen. In this case, the P-wave was correlated against the shear strength of the stabilized soil specimens. For the dimensioning of the lime/cement columns, the values of shear strength of the material were used. Various binder recipes were assessed for shear strength of soil specimens obtained after a certain curing time. The connection between the P-wave velocity and the compressive strength is indirect and material-dependent, i.e., based on the composition of the soil material. A correlation between the S-wave velocity and shear strength of the stabilized soil is reported in Fig. 12a.

a)

b)
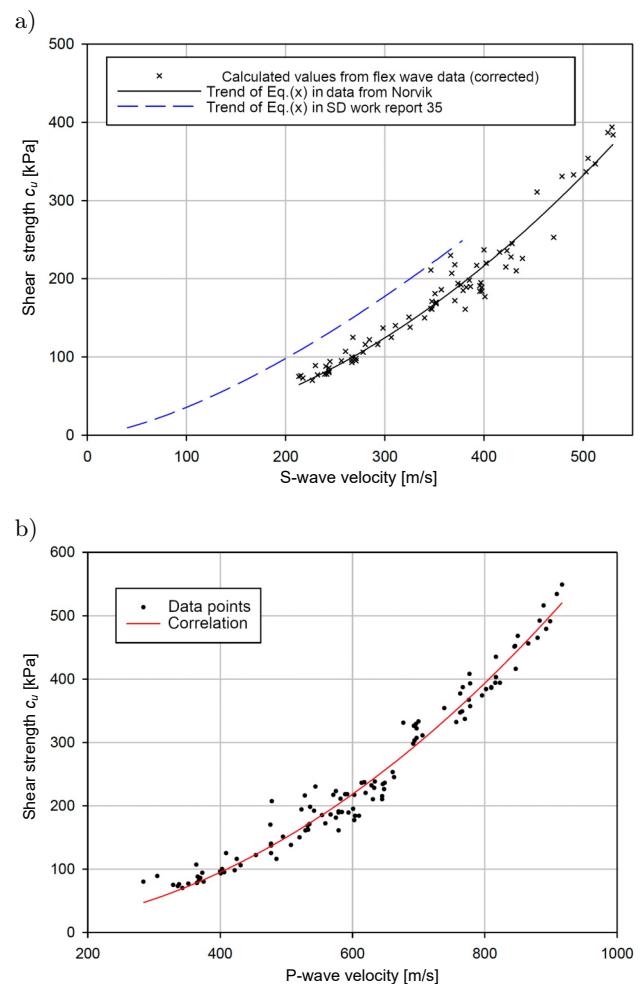
Fig. 12. Shear strength as a function of: a) S-wave speed for stabilized clay from Norvik; b) P-wave rate for stabilized Norvik samples.

Here, the shear wave velocity is adjusted according to Eqs. (6) and (7) (VERÁSTEGUI-FLORES *et al.*, 2015):

$$\tau_{fu} = 0.0424 \times V_s^{1.462}, \tag{6}$$

$$\tau_{fu} = 0.0021 \times V_s^{1.9244}. \tag{7}$$

Here Eq. (6) comes from a reference data using Report 35, and Eq. (7) comes from the data investigation

using stabilized clay from Norvik. The results from the above measurements can be used for the shear strength prediction based on measured P- and S-wave velocities from the in situ measurements, e.g., with down hole measurements. For the Norvik project, the major measurements were the P-waves where a correlation between the P-wave velocity and the shear strength of the soil samples was evaluated and presented in Fig. 12b. The relationship between the P-wave and shear strength corresponds to Eq. (8):

$$\tau_{fu} = 0.0004 \times V_p^{2.0497}. \tag{8}$$

To make a correct comparison between the different stabilized soil samples solidified with varying curing ages, the ambient temperature was taken into account. Thus, in the laboratory tests, the specimens were stored in the climate rooms with a constant temperature maintained at 7°C, where exothermic energy from specimens is cooled away, which affected strength development in soil. In contrast, the temperature in the field is significantly higher due to the less effects from cooling.

The temperature in the field also depends on the amount and type of binder. The comparison between the samples hardened at different temperatures is most appropriately done using the maturity numbers. In Fig. 13, the P-path measurements are reported as a function of curing time and recalculated to the maturity numbers on soil samples cured in 7 and 20°C. In the calculation of the maturity rate (Eq. (5)), the K factor was set to 0.55 by the empirical fitting. Figure 13 shows the differences in the evaluated strength between the samples cured in the laboratory conditions with those from the in-situ field measurements before the final strength is achieved. In the Norvik project, no temperature measurements were carried out in the field. The degree days were used as measurement parameters of curing progress of soil hardening to replace the maturity numbers.
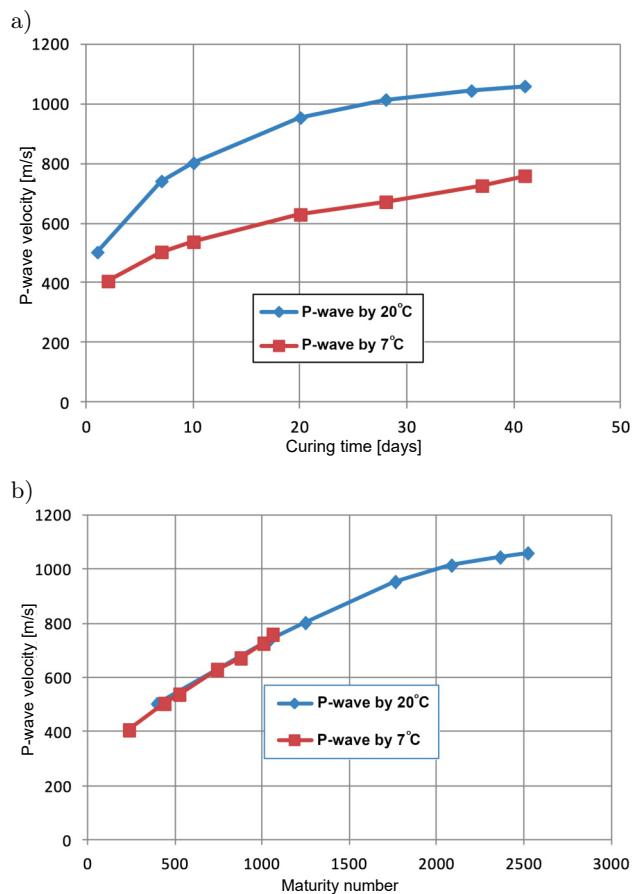
Fig. 13. P-wave rate as a function of: a) the curing time; b) the maturity number (M_T).

3.2. CPT soundings

The results from the CPT soundings are reported in Figs. 17–22. In total, 7 different lime/cement columns with a varying curing age between 9 days and 49 days were examined. The data for the investigated columns are summarised in Table 1. Here the drilling below the column refers to the penetration level of the tool, which is 0.8 meters below the stabilised part. This is

Table 1. Compilation of data from probed columns.

Column ID	Top level of column	Bottom level of column	Stabilized column length for binder LC/SC 50 kg	Drilling below column [m]	Average binder content [kg/m]	Lifting speed [mm/revolution]	Production date	SCPT date	Curing time [days]
ACS155	−0.9	−25.1	24.2	0.8	51.0	20	2016.10.12	2016.11.08	26
ACW151	−0.7	−24.2	23.5	0.8	50.3	20	2016.10.11	2016.11.08	28
ADA147	−0.7	−24.2	23.5	0.8	50.2	20	2016.10.10	2016.11.08	28
ADC148	−0.6	−24.2	23.6	0.8	50.0	20	2016.10.10	2016.11.09	29
AEA358	0.1	−12.0	12.1	0.8	50.5	20	2016.10.31	2016.11.09	9
AEG35	−0.5	−11.5	11.0	0.8	51.1	20	2016.09.19	2016.11.07	49
AEE356	–	–	–	–	–	–	–	2016.11.10	–

due to the fact that the mixing tool releases the binder above the bottom of the tool and normally it is not as much as 0.8 meters. The rise indicates the lifting, or the ascend speed of the tool for each revolution while drilling cycle.

Since there are significant uncertainties related to the evaluation of shear strength of the stabilized soil based on the peak pressure or the pore pressure evaluated from the CPT sounding, this study includes the comparison of the standardised values between the peak pressure q_c and standardised results from seismic measurements. The normalisation was carried out by dividing the results by the largest value. Seismic measurements were recorded in the three lines, of which x- and y-lines represent shear wave measurements and z-line represent the compression wave measurements. The evaluations are reported in Figs. 17–22.

The measured parameters for the lime/cement columns are reported in Fig. 14. The results show a large variation and a very low tip resistance at the depth

[Fig. 14a-f]

g)
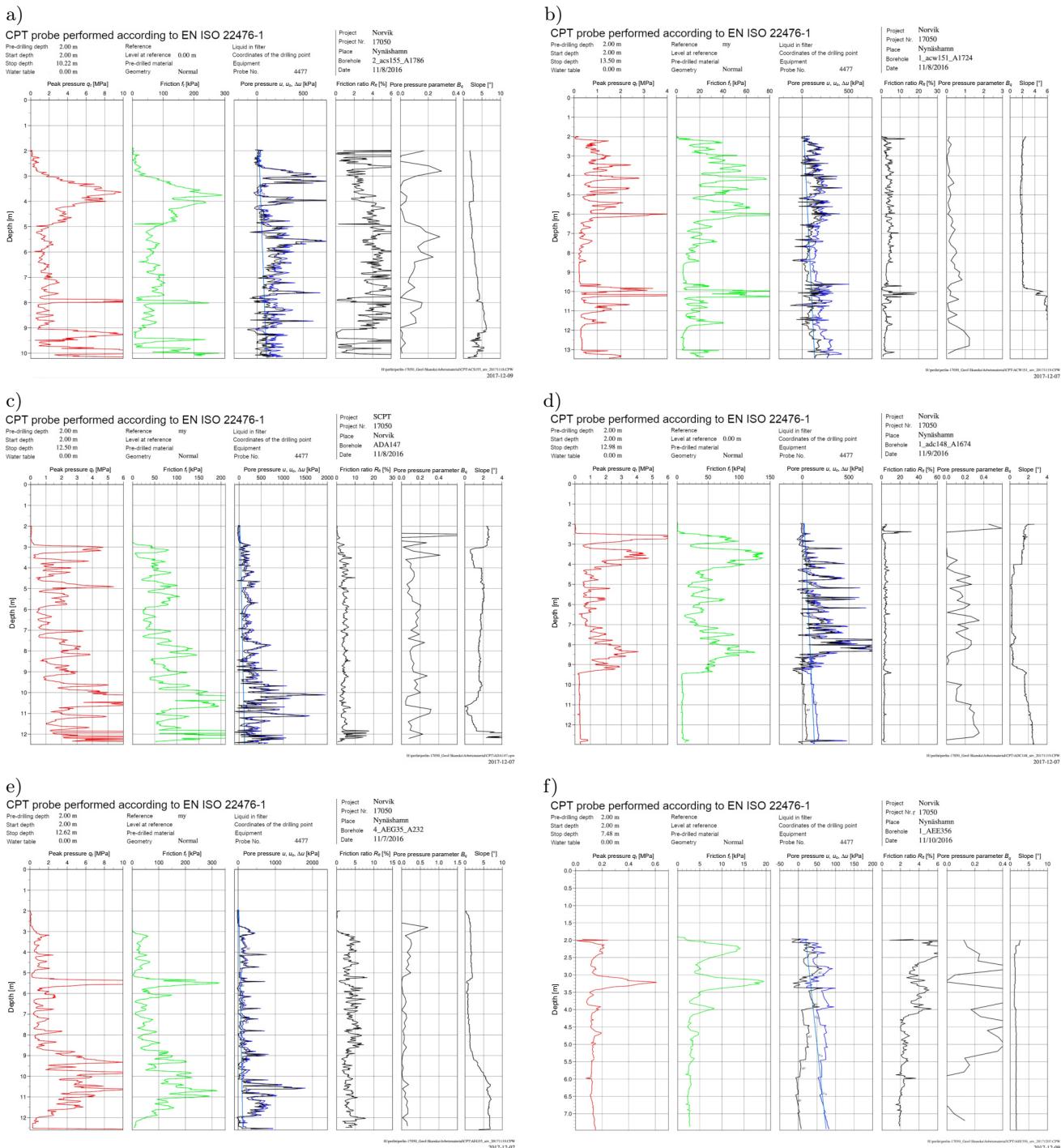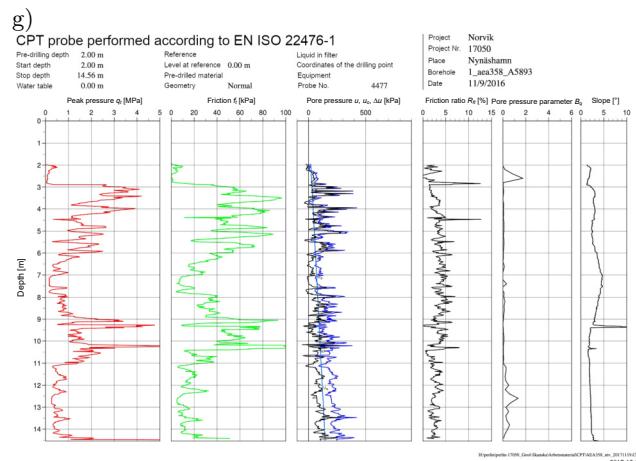
Fig. 14. Evaluated results from the CPT probing of the lime/cement columns (start and end depths of the seven test columns): a) ACS155 (2.00–10.22 m); b) ACW151 (2.00–13.50 m); c) ADA147 (2.00–12.50 m); d) ADC148 (2.00–12.98 m); e) AEG35 (2.00–12.62 m); f) AEE356 (2.00–7.48 m); g) AEA358 (2.00–14.56 m).

between 2 and 2.5 m below the ground surface, after which the tip pressure increases up to about 10 MPa at the level of 3.5 m. Between 5 and 8 m, the peak pressure reaches values of 1–3 MPa; at 8 m of depth it rises steeply to over 10 MPa. The sounding was interrupted at the depth of 10 m due to the stop caused by a high tip pressure. The measured friction shows the consistent results, although with some delay at the end of the probe. The results from seismic measurements show a good agreement between the shear waves in the x- and y-directions.

However, the high peak pressure around the level of 3.5 m is not achieved. The compression wave shows

a better agreement with the peak pressure and the evaluated P-wave velocities for various columns, see Fig. 15. The P-wave velocity down to the level of 7 m is within the compression wave velocities measured in the laboratory, see Fig. 17a and Fig. 12b. The values are, however, quite high, especially considering that the curing age of the column at the time of probing was only 26 days.

The measured shear wave speed for the columns is reported in Figs. 17 to 22 for various directions. The graph shows the results from the evaluated shear wave excited from both right and left in x-direction, the means of signals. The results show generally low

a)

b)

[Fig. 15ab]

c)

d)

e)

f)
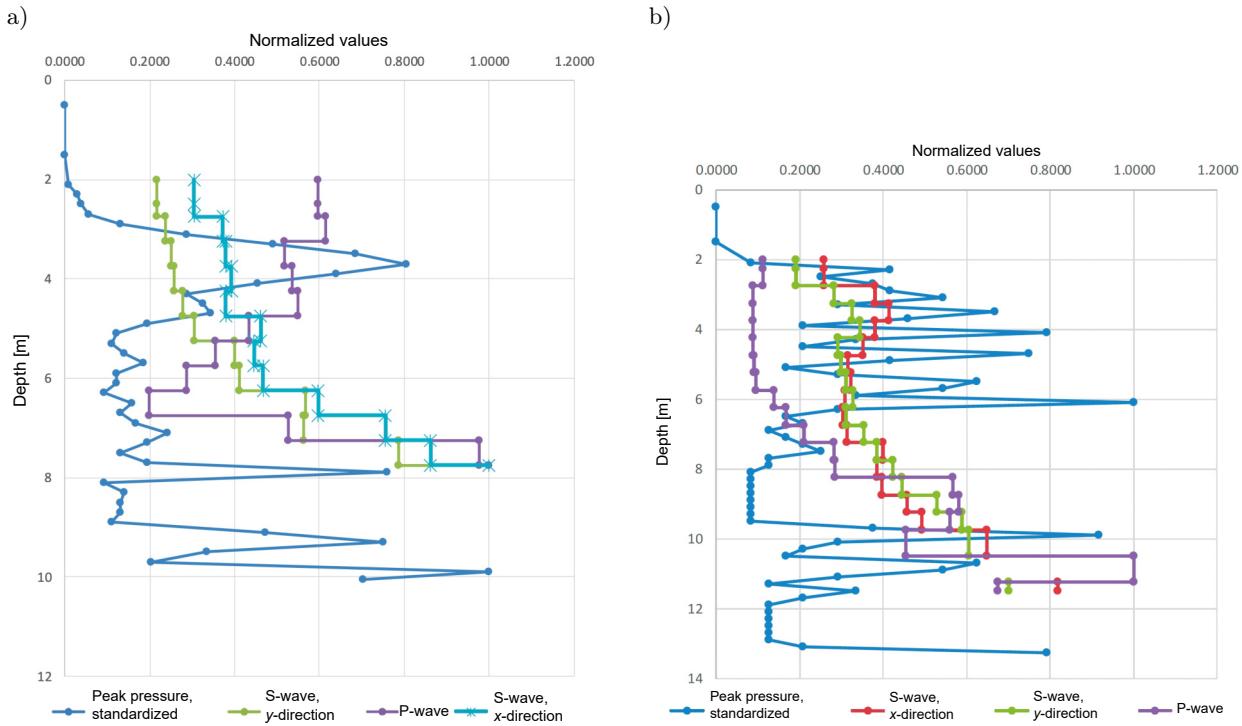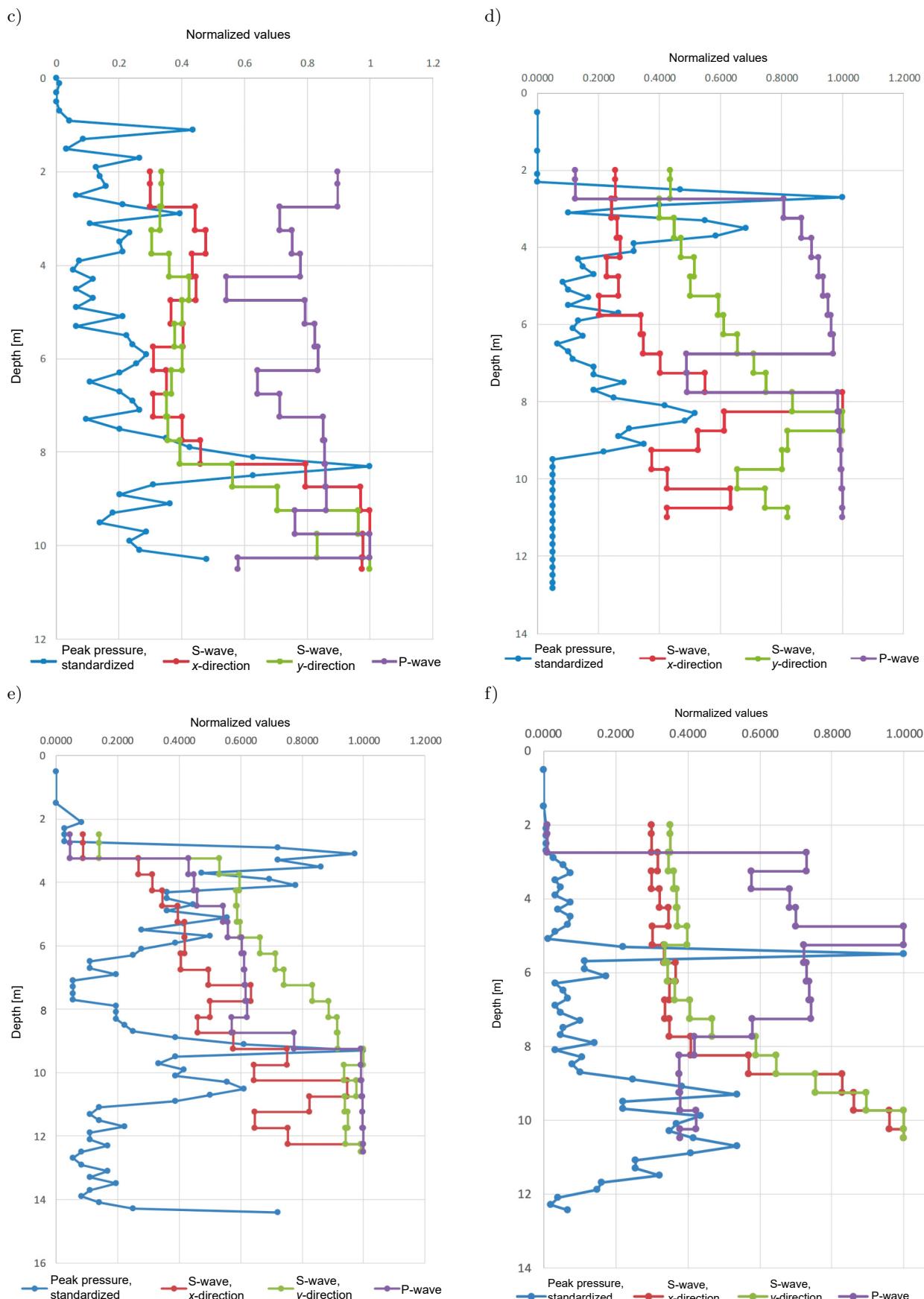
Fig. 15. Normalized peak pressure, S-wave and P-wave for the lime/cement columns: a) ACS155; b) ACW151; c) ADA147; d) ADC148; e) AEA358; f) AEG35

Table 2. Table showing evaluated results from seismic CPT for column ACS155.

Depth [m]	P-wave [m/s]	Ext. c_u from P-wave [kPa]	S-wave, x-dir. [m/s]	S-wave, y-dir. [m/s]	S-wave mean [m/s]	Ext. c_u from S-wave [kPa]
2.25	852	406	98.94	105.27	102.11	15
2.75	877	431	121.06	115.52	118.29	20
3.25	739	303	123.13	122.65	122.89	22
3.75	766	326	127.60	125.87	126.74	23
4.25	785	343	123.17	135.54	129.36	24
4.75	620	212	149.97	158.20	149.09	32
5.25	507	140	144.83	194.82	169.83	41
5.75	410	91	152.01	200.14	176.08	44
6.25	284	43	194.30	276.78	235.54	77
6.75	750	313	245.61	274.35	259.98	93
7.25	1395	1115	280.15	383.49	331.82	149
7.75	1427	1169	325.17	488.08	406.63	220

shear wave velocities. Table 2 shows P- and S-wave velocities for column ACS155. The table also contains calculated shear strength values based on the correlation determined in the laboratory. It is clear that the soil strength evaluated using P-wave measurements is relatively high with values above the actual strength, while strength evaluated using S-wave measurements shows values clearly below the expected results. Down to a depth of 6 m, the evaluated strength values are only slightly above the initial strength values of natural clay. Figure 14 shows the results of testing various columns. These results in the column ACS155 (Fig. 14a) indicate a significant difference compared to a probing in natural clay, cf., Fig. 14f in the column AEE356. The results from the probing of column ACS155 indicate that based on the seismic CPT sounding, the soil has been reinforced with a very solid part around 3.5 m below the ground surface.

The evaluated CPT sounding for the column ACW151 is reported in Fig. 14b. The peak pressure varies from <0.5 MPa to >4 MPa. This may appear to be low for a column that was cured during 28 days at the time of probing. For the column ACW151, the standardised values between the peak pressure, P- and S-wave show rather poor agreement, see Fig. 15b. The evaluated S-wave here gives a fairly good agreement between the x- and y-directions, but does not follow the results from the peak pressure. The highest evaluated P-wave velocity is almost 5000 m/s, which is in parity with the velocities in steel columns. The probing results from the CPT of the column ADA147 are reported in Fig. 14c. Here the tip pressure varies from about 0.5 MPa up to over 6 MPa. This shows a very large variation in strength and indicates difficulties in assessing the strength of a column based on the CPT. Figure 15c shows the standardised values for

the column ADA147. The shear wave velocities show low strength values, Fig. 21. Seismic testing gives bulk modulus values which do not have large variations in the peak pressure but rather an average value. The correlation between the peak pressure and shear wave velocities is low. The evaluated compression wave speed shows values above 2000 m/s.

The column ADC148 also shows large variations in the measured tip pressure. The CPT appears to have exited the column about 9 m below the ground surface, Fig. 14d. This column shows an abnormally large difference in the shear wave between the values measured in x-direction and y-direction. Neither the S- nor P-wave velocities show a good agreement with the tip resistance, Fig. 15d. The P-wave velocities here vary between 1000 and 2000 m/s which does not reflect the expected strength. The sounding result from the column AEA358 shows a similar pattern to the other columns, Fig. 14g. The peak pressure here shows very low values at 7.5 m of depth. The evaluated shear wave velocities here give the credible values of shear strength, c.m.f., Fig. 20, but does not reflect the variation in the peak pressure, Fig. 15e. The test results for column AEG35 are reported in Fig. 14e. This sounding also shows large variations in the tip pressure, which makes it difficult to find a connection between the CPT sounding results and the shear wave velocities, Fig. 15f.

4. Conclusion

The laboratory testing showed a high repeatability between the trials of seismic measurements. The variation in values of the compressive strength and shear strength slightly increased during the period of soil stabilization and increased strength of soil. This

is explained by minor defects and inaccuracies in the test specimens which have a greater effect on strength and result in higher resistance. The results from the field tests show large variations in the tip resistance, but also large variations in shear and compression wave velocities. These results were partly expected but the hypothesis was to find the same trends in the peak pressure and in seismic results. At the seismic CPT, there are several uncertainty factors regarding the seismic measurements which will be investigated in further steps of research. These include the question of how the generated S- and P-waves are transmitted to the column and whether there are cross signals originating from other sources of vibration. Further, the issues include the investigation of how well shear and compression waves are generated at greater depths, and to precise the position of probe within the column.

Seismic CPT has many advantages over the traditional CPT. To ensure that the CPT probe is in the column, a resistivity CPT can be connected there because the stabilized soil has a much lower resistivity due to free ions. One of the great advantages of seismic CPT is that it enables to measure the compressive strength and to apply seismic measurements as determination of the P- and S-wave velocities. Another important parameter for seismic CPT is the financial costs of the works and technical equipment. Here, both a drilling rig and a special expensive equipment are required. This results in the fact that this method is currently quite time-consuming and financially costly. By using a better signal source in seismic methods, some of the disadvantages of the methods can be eliminated. Therefore, this methodology can be a way to evaluate the effects of the lime/cement columns but cannot compete in terms of cost with the limestone column probes.

References

1. Abbiss C.P. (1981), Shear wave measurements of the elasticity of the ground, *Géotechnique*, **31**(1): 91–104, doi: 10.1680/geot.1981.31.1.91.

2. Åhnberg H. (2003), Measured permeabilities in stabilized Swedish soils, [in:] *Third International Conference on Grouting and Ground Treatment*, pp. 622–633, doi: 10.1061/40663(2003)34.

3. Åhnberg H., Holm G. (1987), On the influence of the curing temperature on the shear strength of lime- and cement-stabilized soil [in Swedish: Om inverkan av härdningstemperaturen påskjuvhållfast- heten hos kalk- och cementstabiliserad jord], *Swedish Geotechnical Institute*.

4. Alvarado G., Coop M. (2012), On the performance of bender elements in triaxial tests, *Géotechnique*, **62**(1): 1–17, doi: 10.1680/geot.7.00086.

5. Amaral M.F., Da Fonseca A.V., Arroyo M., Cascante G., Carvalho J. (2011), Compression and shear wave propagation in cemented-sand specimens, *Géotechnique Letters*, **1**(3): 79–84, doi: 10.1680/geolett.11.00032.

6. Archeewa E., Puppala A.J., Saride S., Kalla S. (2011), Numerical model studies of deep soil mixing (DSM) column to mitigate bridge approach settlements, [in:] *Geo-Frontiers Congress 2011*, pp. 3286–3295.

7. Avci E., Mollamahmutoğlu M. (2016), UCS Properties of superfine cement–grouted sand, *Journal of Materials in Civil Engineering*, **28**(12): 06016015, doi: 10.1061/(ASCE)MT.1943-5533.0001659.

8. Bache B.K.F., Wiersholm P., Paniagua P., Emdal A. (2022), Efect of temperature on the strength of lime–cement stabilized Norwegian clays, *Journal of Geotechnical and Geoenvironmental Engineering*, **148**(3): 04021198, doi: 10.1061/(ASCE)GT.1943-5606.0002699.

9. Benz Navarrete M.A., Breul P., Gourvès R. (2022), Application of wave equation theory to improve dynamic cone penetration test for shallow soil characterisation, *Journal of Rock Mechanics and Geotechnical Engineering*, **14**(1): 289–302, doi: 10.1016/j.jrmge.2021.07.004.

10. Bergado D.T., Jamsawang P., Tanchaisawat T., Lai Y.P., Lorenzo G.A. (2008), Performance of reinforced load transfer platforms for embankments supported by deep cement mixing piles, [in:] *GeoCongress 2008: Geosustainability and Geohazard Mitigation*, pp. 628–637.

11. BIN-SHAFIQUE S., RAHMAN K., AZFAR I. (2011), The effect of freezing-thawing cycles on performance of fly ash stabilized expansive soil subbases, [in:] *Advances in Geotechnical Engineering*, pp. 697–706.

12. BISHT V., SALGADO R., PREZZI M. (2021), Material point method for cone penetration in clays, *Journal of Geotechnical and Geoenvironmental Engineering*, **147**(12): 04021158, doi: 10.1061/(ASCE)GT.1943-5606.0002687.

13. BROUWER J.J.M. (2007), *In-situ Soil Testing*, IHS BRE Press.

14. CHAND S.K., SUBBARAO C. (2007), In-place stabilization of pond ash deposits by hydrated lime columns, *Journal of Geotechnical and Geoenvironmental Engineering*, **133**(12): 1609–1616, doi: 10.1061/(ASCE)1090-0241(2007)133:12(1609).

15. CHEN Y., ZHOU Y., KONG G., CHEN L., CHEN G. (2021), Settlement and stress analysis of soil–cement column-reinforced foundation under an in situ stabilized layer, *International Journal of Geomechanics*, **21**(12): 06021032, doi: 10.1061/(ASCE)GM.1943-5622.0002205.

16. COLOMBERO R., KONTOE S., FOTI S., POTTS D.M. (2015), Numerical modelling of wave attenuation through soil, [in:] *Geotechnical Engineering for Infrastructure and Development*, pp. 3959–3964.

17. EL-RAWI N.M., AWAD A.A. (1981), Permeability of lime stabilized soils, *Transportation Engineering Journal of ASCE*, **107**(1): 25–35, doi: 10.1061/TPEJAN.0000907.

18. ELSWORTH D., LEE D.S., HRYCIW R., SHIN S. (2006), Pore pressure response following undrained uCPT sounding in a dilating soil, *Journal of Geotechnical and Geoenvironmental Engineering*, **132**(11): 1485–1495, doi: 10.1061/(ASCE)1090-0241(2006)132:11(1485).

19. ERIKSSON H. (2015), *Personal and written communication with Håkan Eriksso*n, Unpublished discussions, Geomind.

20. FITZGERALD M., ELSWORTH D. (2012), Liquefaction resistance recovered from "on-the-fly" CPTu-measured pore pressures, [in:] *Processing of the Geotechnical Earthquake Engineering and Soil Dynamics Congress IV*, doi: 10.1061/40975(318)69.

21. FOTI S., LAI C.G., LANCELLOTTA R. (2002), Porosity of fluid-saturated porous media from measured seismic wave velocities, *Géotechnique*, **52**(5): 359–373, doi: 10.1680/geot.2002.52.5.359.

22. FOTI S., LANCELLOTTA R. (2004), Soil porosity from seismic velocities, *Géotechnique*, **54**(8): 551–554, doi: 10.1680/geot.2004.54.8.551.

23. GARCIA-SUAREZ J., SEYLABI E., ASIMAKI D. (2021), Seismic harmonic response of inhomogeneous soil: Scaling analysis, *Géotechnique*, **71**(5): 392–405, doi: 10.1680/jgeot.19.P.042.

24. GUAN Z., WANG Y., ZHAO T. (2022), Adaptive sampling strategy for characterizing spatial distribution of soil liquefaction potential using cone penetration test, *Journal of Rock Mechanics and Geotechnical Engineering*, **14**(4): 1221–1231, doi: 10.1016/j.jrmge.2022.01.011.

25. HEIDARIZADEH Y., LAJEVARDI S.H., SHARIFIPOUR M. (2021), Correlation between small-strain shear stiffness and compressive strength of clayey soils stabilized with cement and Nano-SiO2, *International Journal of Geosynthetics and Ground Engineering*, **7**: 12, doi: 10.1007/s40891-021-00258-x.

26. HEPTON P. (1989), Shear wave velocity measurements during penetration testing, [in:] *Penetration testing in the UK*, pp. 275–278, The Institution of Civil Engineers.

27. HEPTON P. (2015), Deep rotary cored boreholes in soils using wireline drilling, [in:] *Advances in Site Investigation Practice*, pp. 269–280, The Institution of Civil Engineers.

28. ITO T., MORI Y., ASADA A. (1994), Evaluation of resistance to liquefaction caused by earthquakes in sandy soil stabilized with quick-lime consolidated briquette piles, *Soils and Foundations*, **34**(1): 33–40, doi: 10.3208/sandf1972.34.33.

29. JAMIOLKOWSKI M., PRESTI D.C.F.L., MANASSERO M. (2003), Evaluation of relative density and shear strength of sands from CPT and DMT, [in:] *Symposium on Soil Behavior and Soft Ground Construction Honoring Charles C. "Chuck" Ladd*, pp. 201–238, doi: 10.1061/40659(2003)7.

30. JEFFERIES M. (2022), On the fundamental nature of the state parameter, *Géotechnique*, **72**(12): 1082–1091, doi: 10.1680/jgeot.20.P.228.

31. JONES R. (1958), In-situ measurement of the dynamic properties of soil by vibration methods, *Géotechnique*, **8**(1): 1–21, doi: 10.1680/geot.1958.8.1.1.

32. KICHOU Z., MAVROULIDOU M., GUNN M.J. (2022), Investigation of the strength evolution of lime-treated London clay soil, [in:] *Proceedings of the Institution of Civil Engineers – Ground Improvement*, doi: 10.1680/jgrim.21.00053.

33. KIM S., GOPALAKRISHNAN K., CEYLAN H. (2012), Moisture susceptibility of subgrade soils stabilized by lignin-based renewable energy coproduct, *Journal of Transportation Engineering*, **138**(11): 1283–1290, doi: 10.1061/(ASCE)TE.1943-5436.0000097.

34. LAMBRECHTS J.R., GANSE M.A., LAYHEE C.A. (2012), Soil mixing to stabilize organic clay for I-95 widening, [in:] *Third International Conference on Grouting and Ground Treatment*, pp. 575–585.

35. LAPOINTE E., FANNIN J., WILSON B.W. (2012), Cement-treated soil: Variation of UCS with soil type, [in:] *Proceedings of the Fourth 502 International Confer-*

ence on Grouting and Deep Mixing, pp. 512–521, doi: 10.1061/9780784412350.0037.

36. LARSSON S. (2017), *Personal communication with Stefan Larsson*, Unpublished discussions, KTH Royal Institute of Technology.

37. LINDH P., LEMENKOVA P. (2021a), Evaluation of different binder combinations of cement, slag and CKD for S/S treatment of TBT contaminated sediments, *Acta Mechanica et Automatica*, **15**: 236–248, doi: 10.2478/ama-2021-0030.

38. LINDH P., LEMENKOVA P. (2021b), Resonant frequency ultrasonic P-Waves for evaluating uniaxial compressive strength of the stabilized slag–cement sediments, *Nordic Concrete Research*, **65**: 39–62, doi: 10.2478/ncr-2021-0012.

39. LINDH P., LEMENKOVA P. (2022a), Dynamics of strength gain in sandy soil stabilised with mixed binders evaluated by elastic P-Waves during compressive loading, *Materials*, **15**(21): 7798, doi: 10.3390/ma15217798.

40. LINDH P., LEMENKOVA P. (2022b), Geochemical tests to study the effects of cement ratio on potassium and TBT leaching and the pH of the marine sediments from the Kattegat Strait, Port of Gothenburg, *Baltica*, **35**: 47–59, doi: 10.5200/baltica.2022.1.4.

41. LINDH P., LEMENKOVA P. (2022c), Impact of strength-enhancing admixtures on stabilization of expansive soil by addition of alternative binders, *Civil and Environmental Engineering*, **18**(2): 726–735, doi: 10.2478/cee-2022-0067.

42. LINDH P., LEMENKOVA P. (2022d), Seismic velocity of P-waves to evaluate strength of stabilized soil for Svenska Cellulosa Aktiebolaget Biorefinery Östrand AB, Timrå, *Bulletin of the Polish Academy of Sciences: Technical Sciences*, **70**(4): e141593, doi: 10.24425/bpasts.2022.141593.

43. LINDH P., LEMENKOVA P. (2022e), Simplex lattice and X-ray diffraction for analysis of soil structure: A case of cement-stabilised compacted tills reinforced with steel slag and slaked lime, *Electronics*, **11**(22): 3726, doi: 10.3390/electronics11223726.

44. LINDH P., LEMENKOVA P. (2022f), Soil contamination from heavy metals and persistent organic pollutants (PAH, PCB and HCB) in the coastal area of Västernorrland, Sweden, *Gospodarka Surowcami Mineralnymi – Mineral Resources Management*, **38**(2): 147–168, doi: 10.24425/gsm.2022.141662.

45. MADHYANNAPU R.S., PUPPALA A.J. (2014), Design and construction guidelines for deep soil mixing to stabilize expansive soils, *Journal of Geotechnical and Geoenvironmental Engineering*, **140**(9): 04014051, doi: 10.1061/(ASCE)GT.1943-5606.0001149.

46. MADHYANNAPU R.S., PUPPALA A.J., BHADRIRAJU V., NAZARIAN S. (2009), Deep soil mixing (DSM) treat-

ment of expansive soils, [in:] *Advances in Ground Improvement: Research to Practice in the United States and China*, pp. 130–139, doi: 10.1061/41025(338)14.

47. MADHYANNAPU R.S., PUPPALA A.J., NAZARIAN S., YUAN D. (2010), Quality assessment and quality control of deep soil mixing construction for stabilizing expansive subsoils, *Journal of Geotechnical and Geoenvironmental Engineering*, **136**(1): 119–128, doi: 10.1061/(ASCE)GT.1943-5606.0000188.

48. MAKUSA G.P., MATTSSON H., KNUTSSON S. (2014), Shear strength evaluation of preloaded stabilized dredged sediments using CPT, [in:] *Proceedings of the 3rd International Symposium on Cone Penetration Testing*, pp. 753–760, http://urn.kb.se/resolve?urn=urn:nbn:se:ltu:diva-35248 (access: 20.12.2022).

49. MCCALLUM A. (2014), A brief introduction to cone penetration testing (CPT) in frozen geomaterials, *Annals of Glaciology*, **55**(68): 7–14, doi: 10.3189/2014AoG68A005.

50. MIRZABABAEI M., ARULRAJAH A., HAQUE A., NIMBALKAR S., MOHAJERANI A. (2018), Effect of fiber reinforcement on shear strength and void ratio of soft clay, *Geosynthetics International*, **25**(4): 471–480, doi: 10.1680/jgein.18.00023.

51. MONTGOMERY D.C. (1996), *Design and Analysis of Experiments*, 7th ed., Wiley.

52. MYERS R.H., MONTGOMERY D.C. (1995), *Response Surface Methodology*, Wiley.

53. OLSEN R.S. (2018), CPT prediction of liquefaction resistance using the CPT soil characterization curve lookup technique, [in:] *Geotechnical Earthquake Engineering and Soil Dynamics V*, pp. 170–181.

54. ORAKOGLU M.E., LIU J., LIN R., TIAN Y. (2017), Performance of clay soil reinforced with fly ash and lignin fiber subjected to freeze-thaw cycles, *Journal of Cold Regions Engineering*, **31**(4): 04017013, doi: 10.1061/(ASCE)CR.1943-5495.0000139.

55. PRICE A.B., DEJONG J.T., BOULANGER R.W., PARRA BASTIDAS A.M., MOUG D. (2016), Effect of prior strain history on the cyclic strength and CPT penetration resistance of silica silt, [in:] *Proceedings of the Geotechnical and Structural Engineering Congress 2016*, pp. 1664–1674.

56. RUSATI P.K., SONG K.-I., YOON Y.-W., HWANG W., LIU L. (2020), Electrical resistivity and elastic wave velocity of sand–cement–inorganic binder mixture, *Environmental Geotechnics*, **7**(5): 318–329, doi: 10.1680/jenge.17.00082.

57. SAFAEE A.M., MAHBOUBI A., NOORZAD A. (2022), Seismic behavior of tiered geogrid reinforced soil (GRS) using treated backfill soil, *Geosynthetics International*, **30**(2): 200–224, doi: 10.1680/jgein.21.00060.

58. SANTAMARINA C., CASCANTE G. (1998), Effect of surface roughness on wave propagation parameters, *Géo-*

technique, **48**(1): 129–136, doi: 10.1680/geot.1998.48.1.129.

59. SAYE S.R., OLSON S.M., FRANKE K.W. (2021), Common-origin approach to assess level-ground liquefaction susceptibility and triggering in CPT-compatible soils using Q, *Journal of Geotechnical and Geoenvironmental Engineering*, **147**(7): 04021046, doi: 10.1061/(ASCE)GT.1943-5606.0002515.

60. SHAHIEN M.M., FAROUK A. (2013), Estimation of deformation modulus of gravelly soils using dynamic cone penetration tests, *Ain Shams Engineering Journal*, **4**(4): 633–640, doi: 10.1016/j.asej.2013.01.008.

61. SHIHATA S.A., BAGHDADI Z.A. (2001), Simplified method to assess freeze-thaw durability of soil cement, *Journal of Materials in Civil Engineering*, **13**(4): 243–247, doi: 10.1061/(ASCE)0899-1561(2001)13:4(243).

62. SONKAR C., MITTAL A. (2022), Evaluation of axial strength of sheathed cold-formed steel wall panels using Rayleigh-Ritz method and direct strength method: Comparative study, *Practice Periodical on Structural Design and Construction*, **27**(1): 04021064, doi: 10.1061/(ASCE)SC.1943-5576.0000623.

63. SULLY J.P., CAMPANELLA R.G. (1991), Effect of lateral stress on CPT penetration pore pressures, *Journal of Geotechnical Engineering*, **117**(7): 1082–1088, doi: 10.1061/(ASCE)0733-9410(1991)117:7(1082).

64. SUNDARY D., MUNIRWAN R.P., AL-HUDA N., MUNIRWANSYAH, SUNGKAR M., JAYA R.P. (2022), Shear strength performance of dredged sediment soil stabilized with lime, *Physics and Chemistry of the Earth, Parts A/B/C*, **128**: 103299, doi: 10.1016/j.pce.2022.103299.

65. TONINI DE ARAÚJO M., TONATTO FERRAZZO S., MANSUR CHAVES H., GRAVINA DA ROCHA C., CESAR CONSOLI N. (2023), Mechanical behavior, mineralogy, and microstructure of alkali-activated wastes-based binder for a clayey soil stabilization, *Construction and Building Materials*, **362**: 129757, doi: 10.1016/j.conbuildmat.2022.129757.

66. TRHLÍKOVÁ J., MAŠÍN D., BOHÁČ J. (2012), Small-strain behaviour of cemented soils, *Géotechnique*, **62**(10): 943–947, doi: 10.1680/geot.9.P.100.

67. VARMA M., MAJI V.B., BOOMINATHAN A. (2022), Seismic assessment of shotcrete support in jointed rock tunnels, *International Journal of Geosynthetics and Ground Engineering*, **8**: 51, doi: 10.1007/s40891-022-00392-0.

68. VERÁSTEGUI-FLORES R.D., DI EMIDIO G., BEZUIJEN A., VANWALLEGHEM J., KERSEMANS M. (2015), Evaluation of the free–free resonant frequency method to determine stiffness moduli of cement-treated soil, *Soils and Foundations*, **55**(5): 943–950, doi: 10.1016/j.sandf.2015.09.001.

69. XU B., YI Y. (2021), Soft clay stabilization using three industry byproducts, *Journal of Materials in Civil Engineering*, **33**(5): 06021002, doi: 10.1061/(ASCE)MT.1943-5533.0003710.

70. YAPAGE N.N.S., LIYANAPATHIRANA D.S., KELLY R.B., POULOS H.G., LEO C.J. (2014), Numerical modeling of an embankment over soft ground improved with deep cement mixed columns: Case history, *Journal of Geotechnical and Geoenvironmental Engineering*, **140**(11): 04014062, doi: 10.1061/(ASCE)GT.1943-5606.0001165.

71. ZHANG Y., DANIELS J.L., CETIN B., BAUCOM I.K. (2020), Effect of temperature on pH, conductivity, and strength of lime-stabilized soil, *Journal of Materials in Civil Engineering*, **32**(3): 04019380, doi: 10.1061/(ASCE)MT.1943-5533.0003062.

Appendix A. An example of the protocol evaluated using Conrad v.3.1

CPT probing carried out according to EN ISO 22476-1
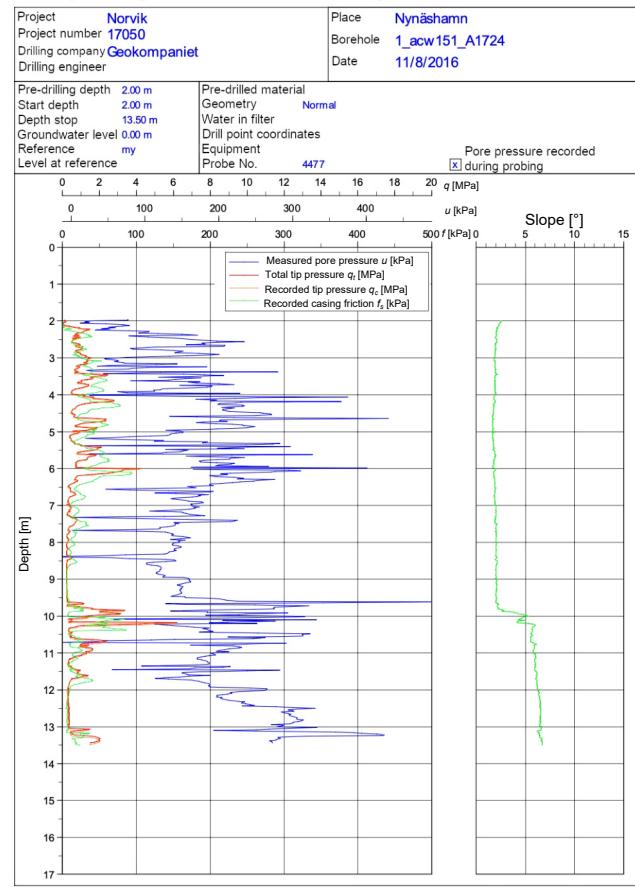
Fig. 16. Protocol with standard scales evaluated using Conrad software, version 3.1.

Appendix B. Supplementary material

a) Borehole: AEG35, *x*-direction – mean signal
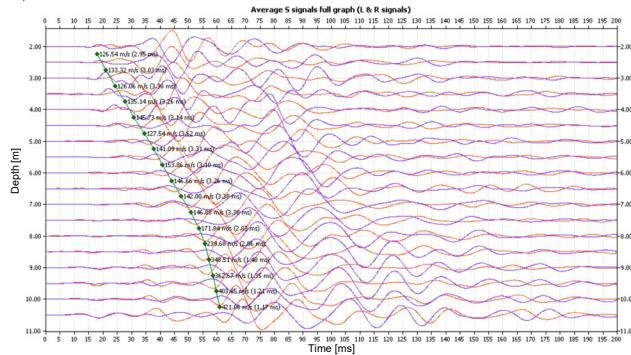
b) Borehole: AEG35, *y*-direction – mean signal
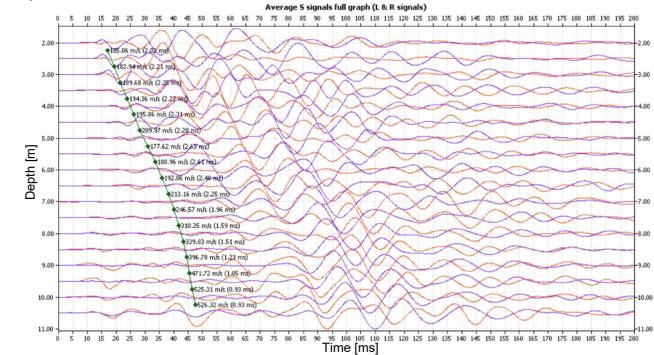
c) Borehole: AEG35, *z*-direction – *p*-signal
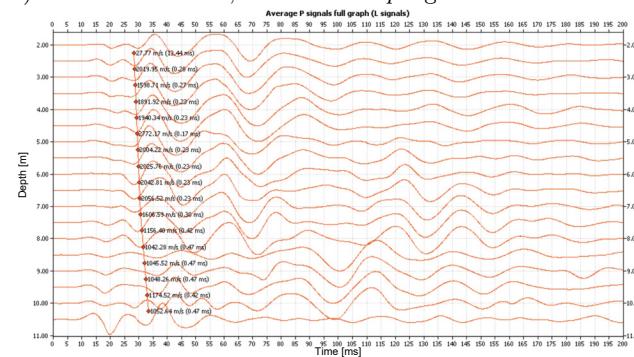
Fig. 17. Signals for AEG35 column.

a) Borehole: ADC148, *x*-direction – mean signal
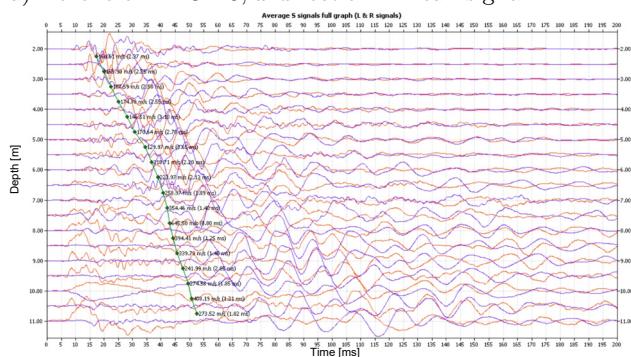
b) Borehole: ADC148, *y*-direction – mean signal
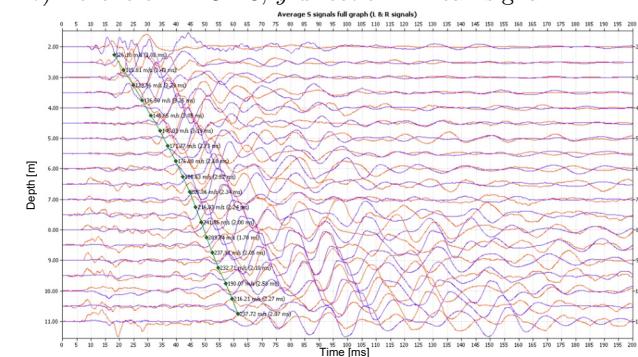
c) Borehole: ADC148, *z*-direction – *p*-signal
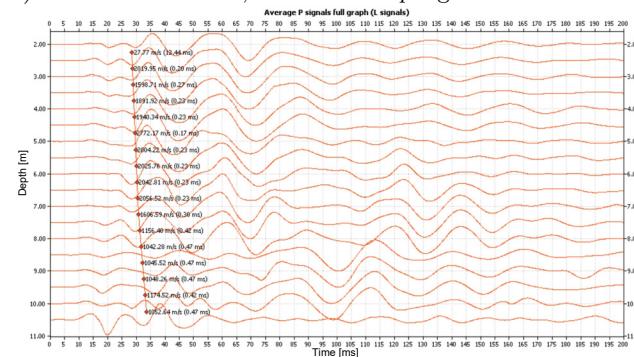
Fig. 18. Signals for ADC148 column.

a) Borehole: ACS155, x-direction – mean signal
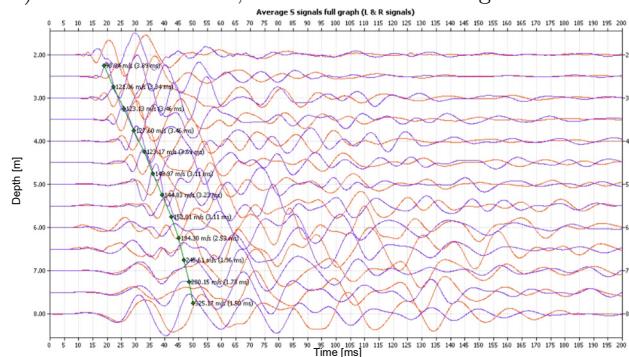
b) Borehole: ACS155, y-direction – mean signal
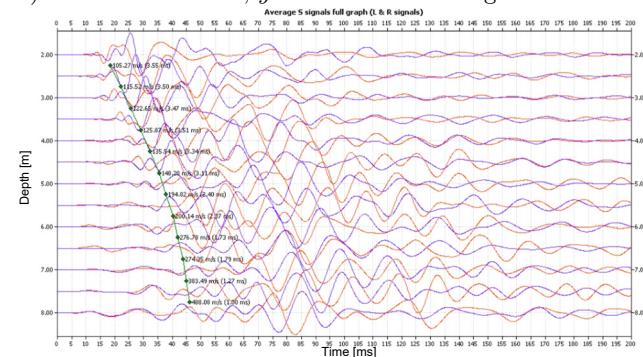
c) Borehole: ACS155, z-direction – p-signal
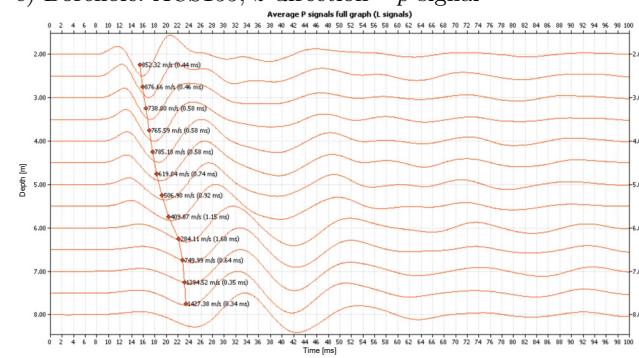
Fig. 19. Signals for ACS155 column.

a) Borehole: AEA358, x-direction – mean signal
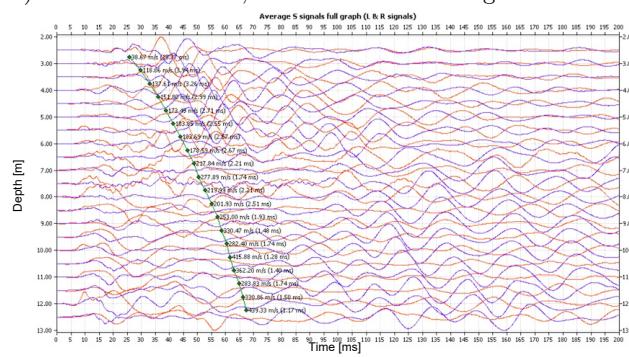
b) Borehole: AEA358, y-direction – mean signal
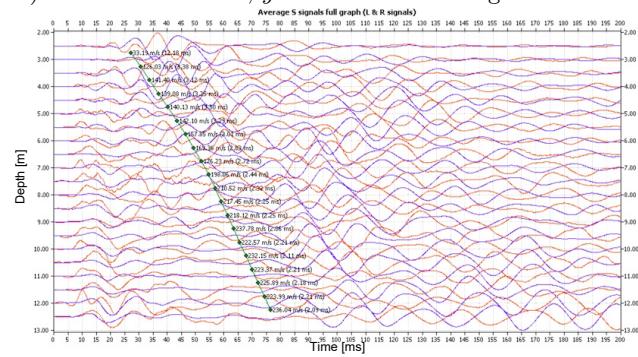
c) Borehole: AEA358, z-direction – p-signal
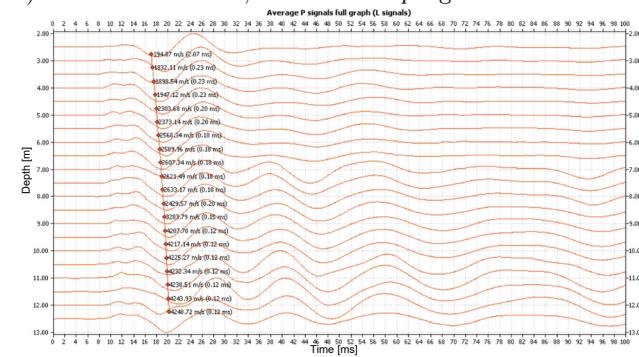
Fig. 20. Signals for AEA358 column.

a) Borehole: ADA147, *x*-direction – mean signal
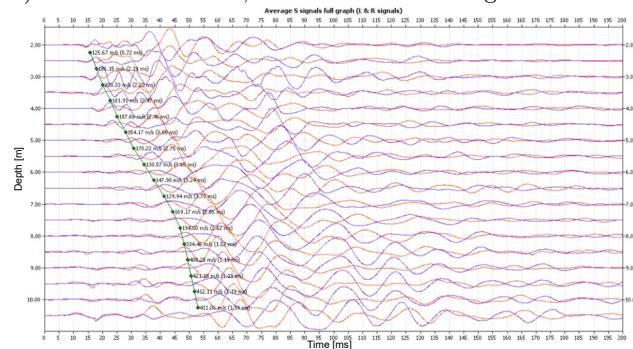
b) Borehole: ADA147, *y*-direction – mean signal
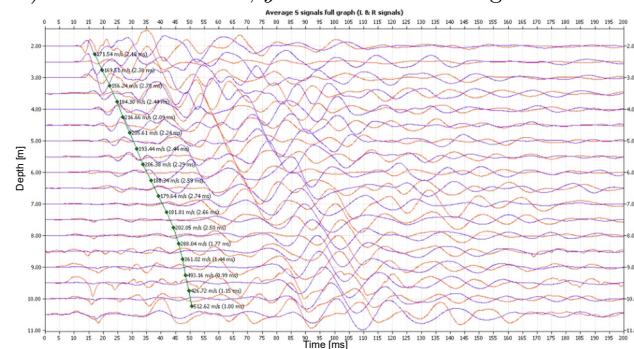
c) Borehole: ADA147, *z*-direction – *p*-signal
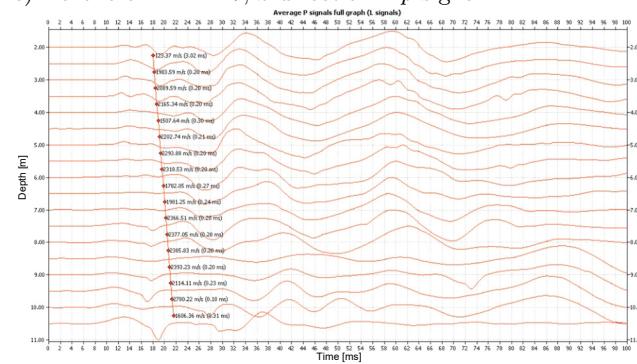
Fig. 21. Signals for ADA147 column.

a) Borehole: ACW151, *x*-direction – mean signal
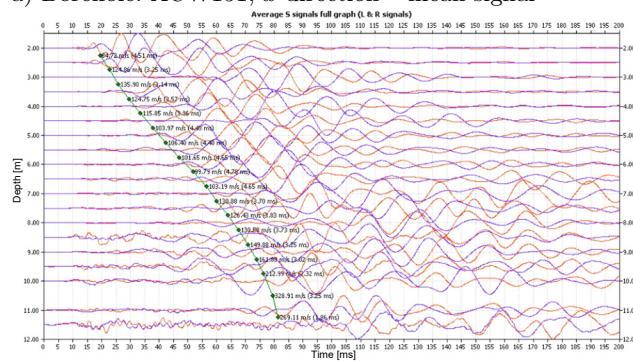
b) Borehole: ACW151, *y*-direction – mean signal
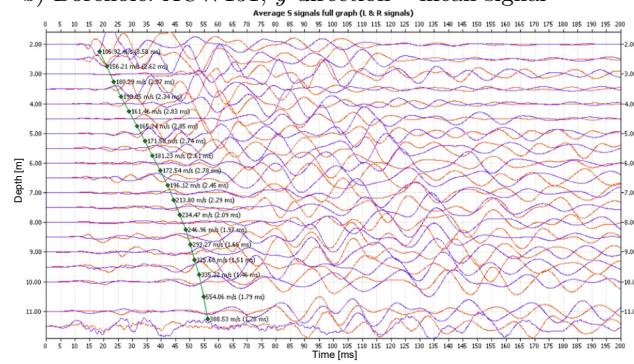
c) Borehole: ACW151, *z*-direction – *p*-signal
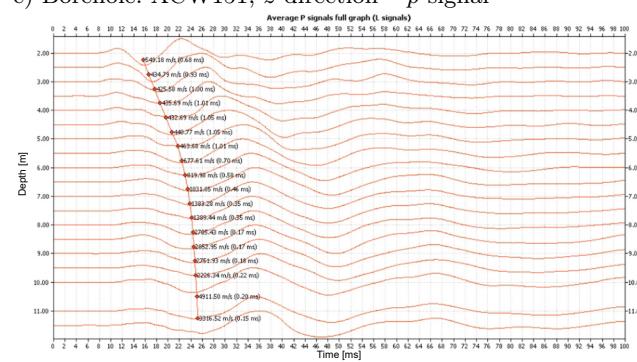
Fig. 22. Signals for ACW151 column.